

Proceedings of the Korean Nuclear Society Spring Meeting
Gyeongju, Korea, May 2003

Non-uniform Flow Characteristics in the Steam Generator U-Tubes During Natural Circulation

J.-J. Jeong, M. Hwang, Y. J. Lee, K. D. Kim, B. D. Chung

Korea Atomic Energy Research Institute
Dukjin 150, Yuseong, 305-600 Daejeon, Korea
E-mail: jjjeong@kaeri.re.kr

Abstract

A one-dimensional, integrated flow model is formulated to analyze single- and two-phase flow characteristics in the primary side of vertical, inverted U-tube steam generators. It is shown that flow excursion instability can exist in the flow inside the U-tubes under certain low-flow conditions. A stability criterion for the flow excursion is derived and its physical interpretation is given. Heterogeneous flow behaviors in multiple U-tubes are also discussed.

1. Introduction

Natural circulation is an essential shutdown decay heat removal mechanism during transients or accidents occurring in pressurized water reactors (PWRs) following loss of forced circulation [1]. The necessary ingredients for natural circulation are a heat source, a heat sink at an elevation above the heat source, and a continuous path between the two. Events leading to natural-circulation cooling include the loss of off-site power, common-mode reactor coolant pump (RCP) failures, and operator termination of forced circulation. The latter, which may occur during a small-break loss-of-coolant accident, is of particular interest because there is a potential for loss of primary coolant inventory caused by larger breaks or when makeup coolant is not provided.

There are three distinct modes of natural circulation in PWR plants having U-tube steam generators (UTSGs): single-phase liquid, two-phase mixture (liquid continuous), and reflux condensation [2, 3]. The occurrence of a given natural circulation mode depends primarily on the primary system mass inventory. In this paper, the primary-side flows (i.e., the flow inside U-tubes) of the UTSG under single-phase and two-phase natural circulation are analyzed.

Generally, a UTSG has several hundreds or thousands of vertical, inverted U-tubes, of which the tube lengths are different. For example, the UTSGs of Kori 3 & 4 and Yonggwang 3 & 4 plants have 5626 and 8214 U-tubes, respectively. In the LSTF facility [2, 3], which is a 1/48 volume-scaled, full-height model of a Westinghouse-type 4-loop PWR, there are 141 U-tubes having 9 different heights and the tube lengths range from 19.04 m to 22.27 m. Under forced-circulation condition, the flow behaviors in these U-tubes are very similar except for

slightly different mass flow rates. Even for natural-circulation condition, it is generally assumed that the flow rates in the U-tubes are almost the same. However, from some experiments under single- or two-phase natural circulations, it is known that flow behaviors in the multiple U-tubes are quite heterogeneous [2 ~ 5]. Kukita *et al.* [2] presented the results of natural circulation experiments conducted in the LSTF facility. The results showed that under certain flow conditions the flow in longer U-tubes was stagnant or reversed in direction, whereas the flow in short tubes was in the normal direction. Non-uniform flow behaviors in the multiple U-tubes were also observed in the BETHSY facility during mid-loop operation experiments [5]. These behaviors might be evoked from static and/or dynamic instabilities.

In Section 2, to analyze the flow characteristics in the U-tubes, a one-dimensional, integrated flow model is formulated. Using the flow model, it is shown that flow excursion instability can exist under certain low-flow conditions. A stability criterion for the flow excursion is derived and its physical interpretation is also given. This flow characteristic evokes non-uniform flow behavior in the multiple U-tubes with different tube lengths. In Section 3, the heterogeneous flow behaviors are discussed. Finally, the conclusions are given in the last section.

2. Flow Characteristic in a U-tube

Figure 1 shows a schematic of the UTSG. In this section, steady-state pressure drop characteristic in a U-tube is derived, which is later used for demonstrating the existence of flow excursions. To derive the pressure drop versus flow rate in a U-tube, it is sufficient to adopt a one-dimensional momentum equation:

$$\frac{\partial(\mathbf{r}U)}{\partial t} + \frac{\partial(\mathbf{r}U^2)}{\partial s} = -\frac{\partial P}{\partial s} - \frac{f}{D_i} \frac{\mathbf{r}U^2}{2} \pm \mathbf{r}g, \quad (1)$$

where s is the coordinate for integration along the U-tube.

Integrating the one-dimensional momentum equation from inlet to exit plenum (see Fig. 2), we obtain the following equation:

$$\frac{L}{A} \frac{d\dot{m}}{dt} = (P_i - P_e) - \frac{1}{2} f \frac{L}{D_i} \frac{|\dot{m}|\dot{m}}{\bar{\mathbf{r}}A^2} - \frac{1}{2} K \frac{|\dot{m}|\dot{m}}{\bar{\mathbf{r}}A^2} - \left(\frac{1}{\mathbf{r}_e} - \frac{1}{\mathbf{r}_i} \right) \frac{\dot{m}^2}{A^2} + g(\bar{\mathbf{r}}_c - \bar{\mathbf{r}}_h)H \quad (2)$$

where $\dot{m} = \mathbf{r}UA$ (mass flow rate in a U-tube),

$\bar{\mathbf{r}}_c$ and $\bar{\mathbf{r}}_h$: average densities for the cold and hot sides of the U-tube, respectively.

The first term in the right-hand side (RHS) of Eq. (2) is total pressure drop between the inlet and exit plenums. The second and third terms are frictional loss and form loss (irreversible loss terms), respectively. The fourth term represents spatial acceleration, which is negligible for the flow inside U-tubes in comparison with other terms. The last term is gravitational head.

For steady state, the total pressure drop can be approximated as:

$$\begin{aligned} \Delta P &= P_i - P_e \\ &= \frac{1}{2} \left(f \frac{L}{D_i} + K \right) \frac{|\dot{m}|\dot{m}}{\bar{\mathbf{r}}A^2} - g(\bar{\mathbf{r}}_c - \bar{\mathbf{r}}_h)H, \end{aligned} \quad (3)$$

where the spatial acceleration term is neglected.

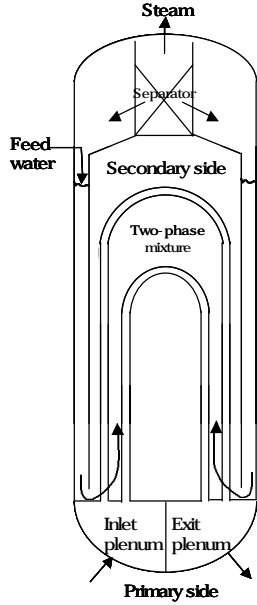


Fig. 1. A schematic of the UTSG.

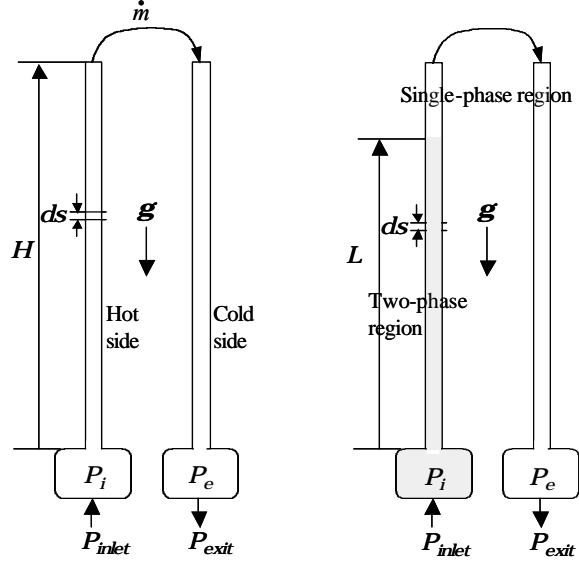


Fig. 2. Primary side modeling: single- and two-phase cases.

To analyze flow characteristics inside the U-tubes, it's necessary to represent the gravitational head in terms of mass flow rate. Hereinafter, for simplicity, it is assumed that the tube height is half the tube length, that is, $H=L / 2$.

2.1 Single-Phase Flow inside the U-tubes

Single-phase liquid flow is considered first. Water density can be approximated as a function of temperature for a small temperature range:

$$\mathbf{r}(T) = \mathbf{r}_o [1 - \mathbf{b}(T - T_o)]. \quad (4)$$

Then, the gravitational head is written as:

$$g(\bar{\mathbf{r}}_C - \bar{\mathbf{r}}_H)H = g\mathbf{r}_o\mathbf{b}H(\bar{T}_H - \bar{T}_C) \quad (5)$$

where \bar{T}_H and \bar{T}_C are average coolant temperatures of hot and cold sides, respectively. Next, to obtain the primary-side coolant temperature distribution in the U-tube, a steady-state energy balance is used. The energy balance for a small differential element of the U-tube shown in Fig. 2 is written as

$$-\dot{m}C_p dT^{pri} = \mathbf{p}D_o U_{If}(T^{pri} - T^{sec})ds \quad (6)$$

where $T^{pri} \geq T^{sec}$.

It is assumed that coolant in the secondary side of the U-tubes is saturated and T_{sec} is uniform in the tube bundle region. The overall heat transfer coefficient U_{If} is also assumed to be uniform along the U-tube. This assumption involves a little error but yields reasonably good approximation to the primary-side temperature profile [6]. Integrating Eq. (6) from the inlet to a certain location s , we obtain the primary-side coolant temperature at the location;

$$T^{pri}(s) = T^{sec} + \Delta T_{If} e^{-(\mathbf{x}/\dot{m})s} \quad (7)$$

where $\Delta T_{1f} = T_{inlet}^{pri} - T^{sec}$,

$$\mathbf{x} = \rho D_o U_{1f} / C_p.$$

Using Eq. (7), \bar{T}_C and \bar{T}_H can be obtained. Inserting them into Eq. (5), Equation (3) is represented as follows:

$$\Delta P \approx \frac{1}{2} \left(f \frac{L}{D_i} + K \right) \frac{|\dot{m}| \dot{m}}{\bar{\mathbf{r}} A^2} - g \mathbf{r}_o \mathbf{b} \Delta T_{1f} \frac{\dot{m}}{\mathbf{x}} \left(1 - e^{-\mathbf{x} / \dot{m} H} \right)^2. \quad (8)$$

2.2 Two-Phase Flow inside the U-tubes

When two-phase mixture enters the U-tube, three flow conditions are possible; (i) vapor is completely condensed in the up flow region, (ii) vapor is completely condensed in the down flow region, and (iii) vapor is not completely condensed even at the exit. In the second and third cases, stable two-phase natural circulation may not continue. In this paper, the first case is considered only and, for simplicity, it is assumed that two-phase flow in the U-tube is homogeneous and equilibrium. Then, the density of two-phase mixture is given as:

$$\mathbf{r}_{2f}(s) = \frac{1}{v_f + x(s)v_{fg}}, \quad (9)$$

where $x(s)$ is the thermal equilibrium quality defined by

$$x(s) = \{h(s) - h_f\} / h_{fg}. \quad (10)$$

Local mixture enthalpy $h(s)$ can be obtained from the energy balance:

$$-\dot{m} dh = \rho D_o U_{2f} (T_{sat}^{pri} - T^{sec}) ds.$$

Thus,

$$h(s) = h_{inlet} - \frac{\rho D_o U_{2f} \Delta T_{2f}}{\dot{m}} s \quad (11)$$

where $s \leq L_{2f} \leq H$,

$$L_{2f} = (\dot{m} x_i h_{fg}) / (\rho D_o U_{2f} \Delta T_{2f}),$$

$$\Delta T_{2f} = T_{sat}^{pri} - T^{sec},$$

$$x_i = (h_{inlet} - h_f) / h_{fg}.$$

From Eqs. (9) and (11), two-phase mixture density can be obtained. For single-phase region, the density is given as

$$\mathbf{r}_{1f}(s) = \mathbf{r}_f^{sec} \left\{ 1 - \mathbf{b} [T^{pri}(s) - T^{sec}] \right\} \quad (12)$$

where $s \geq L_{2f}$,

$$T^{pri}(s) = T^{sec} + \Delta T_{2f} e^{-(\mathbf{x} / \dot{m})(s - L_{2f})}.$$

Using Eqs. (9) through (12), $\bar{\mathbf{r}}_H$ and $\bar{\mathbf{r}}_C$ are obtained:

$$\begin{aligned} \bar{\mathbf{r}}_H &= \left\{ \int_0^{L_{2f}} \mathbf{r}_{2f}(s) ds + \int_{L_{2f}}^H \mathbf{r}_{1f}(s) ds \right\} / H \\ &= \frac{\dot{m} h_{fg}}{H \rho D_o U_{2f} \Delta T_{2f} v_{fg}} \log \left(1 + \frac{v_{fg}}{v_f} x_i \right) + \mathbf{r}_{f,sat}^{sec} \left\{ 1 - \frac{\mathbf{b} \Delta T_{2f} \dot{m}}{(H - L_{2f}) \mathbf{x}} \left(1 - e^{-(\mathbf{x} / \dot{m})(H - L_{2f})} \right) \right\} \frac{H - L_{2f}}{H}, \quad (13) \\ \bar{\mathbf{r}}_C &= \int_H^{2H} \mathbf{r}_{1f}(s) ds / H \end{aligned}$$

$$= \mathbf{r}_{f, \text{sec}}^{sat} \left\{ 1 - \frac{\mathbf{b}\Delta T_{2f} \dot{m}}{H\mathbf{x}} e^{-(\mathbf{x}/\dot{m})(H-L_{2f})} (1 - e^{-(\mathbf{x}/\dot{m})H}) \right\}. \quad (14)$$

For two-phase flow, the irreversible loss terms can be approximated as follows:

$$\begin{aligned} \Delta P_{irrev} &= \Delta P_{fric}^{2f} + \Delta P_{fric}^{1f} + \Delta P_{form}^{1f} \\ &= \frac{1}{2} f \frac{L_{2f}}{D_i} \frac{\dot{m}^2}{\bar{\mathbf{r}}_{2f} A^2} + \frac{1}{2} f \frac{L-L_{2f}}{D_i} \frac{\dot{m}^2}{\bar{\mathbf{r}}_{1f} A^2} + \frac{K}{2} \frac{\dot{m}^2}{\bar{\mathbf{r}}_{1f} A^2} \\ &= \frac{1}{2} \left\{ f \frac{L}{D_i} + K \right\} \frac{\dot{m}^2}{\bar{\mathbf{r}}_{1f} A^2} + \frac{f x_i h_{fg}}{2 \mathbf{p} D_i D_o U_{2f} \Delta T_{2f}} [\bar{\mathbf{r}}_{1f} (v_f + 0.5 x_i v_{fg}) - 1] \frac{\dot{m}^3}{\bar{\mathbf{r}}_{1f} A^2} \end{aligned} \quad (15)$$

In Eq. (15), it is assumed that the form loss occurs in the single-phase region only. Inserting Eqs. (13) through (15) into Eq. (3) yields

$$\begin{aligned} \Delta P &\cong \frac{1}{2} \left(f \frac{L}{D_i} + K \right) \frac{\dot{m}^2}{\bar{\mathbf{r}}_{1f} A^2} + \frac{f x_i h_{fg}}{2 \mathbf{p} D_i D_o U_{2f} \Delta T_{2f}} [\bar{\mathbf{r}}_{1f} (v_f + 0.5 x_i v_{fg}) - 1] \frac{\dot{m}^3}{\bar{\mathbf{r}}_{1f} A^2} \\ &\quad - \frac{\mathbf{g} \mathbf{r}_f^{sec} \mathbf{b} \Delta T_{2f} C_p}{\mathbf{p} D_o U_{1f}} \left[1 - 2 e^{-(\mathbf{x}/\dot{m})(H-L_{2f})} + e^{-(\mathbf{x}/\dot{m})(2H-L_{2f})} \right] \dot{m} \\ &\quad - \frac{\mathbf{g} h_{fg}}{\mathbf{p} D_o U_{2f} \Delta T_{2f}} \left[x_i \mathbf{r}_f^{sec} - \frac{1}{v_{fg}} \log \left(1 + \frac{v_{fg}}{v_f} x_i \right) \right] \dot{m} \end{aligned} \quad (16)$$

The first and second terms in the RHS of Eq. (16) are single- and two-phase frictional pressure losses. The third and fourth terms represent the gravitational head. It is noted that Eq. (8) is a particular case of Eq. (16); that is, if inlet quality x_i in Eq. (16) is zero, Eq. (16) is reduced to Eq. (8).

2.3 Flow Excursions

Both Eq. (8) and Eq. (16) represent the total pressure drop as a function of mass flow rate. They show that the gravitational head initially decreases and asymptotically converges to a certain value (zero in the case of single-phase flow) as the mass flow increases, whereas the irreversible loss increases nonlinearly as the mass flow increases. Due to the competing effect of the two terms, total pressure drop decreases with increasing flow *under low-flow condition* as can be seen in Fig. 3, and has a minimum at point **A**. Due to the flow characteristic, a flow excursion can occur at point **A**.

Considering negative-direction flow, the pressure drop curve can be depicted as in Fig. 4. If we gradually decrease the pressure drop (initially from point **S** in Fig. 4), the flow rate will be also decreased gradually. However, reaching point **A** in Fig. 4, a flow excursion will occur, that is, the flow suddenly changes from point **A** to point **B**. This is a typical flow excursion instability. It is noted that, at point **A**, the slope of pressure drop-flow rate curve is zero.

This flow excursion can be easily explained by using a linear perturbation analysis [7]. Lets consider the single-phase case first. Using Eq. (8), Equation (2) can be written as:

$$\frac{L}{A} \frac{d\dot{m}}{dt} \approx (P_i - P_e) - \frac{1}{2} \left(f \frac{L}{D_i} + K \right) \frac{|\dot{m}| \dot{m}}{\bar{\mathbf{r}} A^2} + \mathbf{g} \mathbf{r}_o \mathbf{b} \Delta T_{1f} \frac{C_p}{U_{1f} \mathbf{p} D_o} \dot{m} (1 - e^{-(\mathbf{x}/\dot{m})H})^2 \quad (17)$$

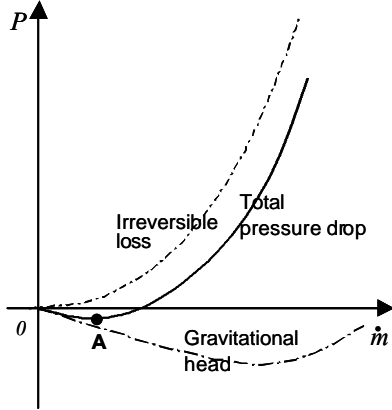


Fig. 3. Pressure drop versus mass flow rate.

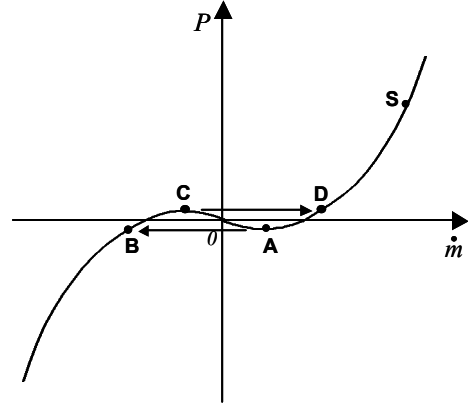


Fig. 4. Flow excursion
(A \rightarrow B; C \rightarrow D).

Equation (17) is valid around an equilibrium point because the steady-state assumption was used for deriving the gravitational head term. However, Equation (17) is still effective for describing transient flow characteristics within a U-tube. Let's simplify Eq. (17) for convenience. The exponent in the RHS of Eq. (17), $(\mathbf{x}/\dot{m})H$, is generally around unity in the U-tubes of typical PWR plants under normal operating condition.¹ However, under low-flow conditions such as natural circulation, the exponent increases because of reduced mass flow rate and, thus, the exponential term in Eq. (17) can be neglected. Then, Equation (17) can be approximated as:

$$\frac{L}{A} \frac{d\dot{m}}{dt} \approx (P_i - P_e) - \frac{1}{2} \left(f \frac{L}{D_i} + K \right) \frac{|\dot{m}|\dot{m}}{\bar{r}A^2} + g r_o b \Delta T_{if} \frac{C_p}{U_{if} p D_o} \dot{m}. \quad (18)$$

Consider, now, small perturbations around an equilibrium point denoted by the subscript o :
 $\dot{m}(t) = \dot{m}_o + \mathbf{d}\dot{m}(t)$.

Substituting this expression into Eq. (18) and eliminating the steady-state terms, we obtain the following governing equation for the flow rate perturbations:

$$\frac{L}{A} \frac{d\mathbf{d}\dot{m}}{dt} = - \left[s_w \left(f \frac{L}{D_i} + K \right) \frac{\dot{m}_o}{\bar{r}A^2} - g r_o b \Delta T_{if} \frac{C_p}{U_{if} p D_o} \right] \mathbf{d}\dot{m} \quad (19)$$

where $s_w = \begin{cases} 1 & \text{if } \dot{m} \geq 0 \\ -1 & \text{if } \dot{m} < 0 \end{cases}$.

In Eq. (19), $\mathbf{d}\dot{m}^2$ term was neglected. The solution of Eq. (19) is given in the form:

$$\mathbf{d}\dot{m}(t) = \mathbf{d}\dot{m}_o e^{-1t} \quad (20)$$

¹ The exponent, $(\mathbf{x}/\dot{m})H$, can be approximated from a steady-state energy balance:

$$\dot{m}_{RCS} C_p (T_H - T_C) = U_{SG} A_{SG} \frac{T_H - T_C}{\log[(T_H - T^{sec})/(T_C - T^{sec})]}$$

Thus, $(\mathbf{x}/\dot{m})H = \frac{1}{2} \log[(T_H - T^{sec})/(T_C - T^{sec})]$

Using the normal operating condition of Kori 3 & 4 nuclear power plant;

$T_H = 599.0$ K, $T_C = 564.8$ K, $T^{sec} = 555.3$ K.

Therefore, $(\mathbf{x}/\dot{m})H = 0.763$.

$$\text{where } \mathbf{I} = \frac{A}{L} \left[s_w \left(f \frac{L}{D_i} + K \right) \frac{\dot{m}_o}{\bar{r} A^2} - g \mathbf{r}_o \mathbf{b} \Delta T_{1f} \frac{C_p}{U_{1f} \rho D_o} \right].$$

Therefore, the system is stable against perturbations *only if* \mathbf{I} is positive. In other words, the primary-side flow is stable if the flow is greater than the threshold value (hereinafter called characteristic flow):

$$|\dot{m}| > \dot{m}_c$$

$$\text{where } \dot{m}_c = \frac{\rho D_i^4 g \mathbf{r}_o \bar{r} \mathbf{b} C_p \Delta T_{1f}}{16 D_o (fL/D_i + K) U_{1f}}. \quad (21)$$

Similarly, the characteristic flow for two-phase case is approximated:

$$\dot{m}_{c,2f} \approx \frac{\rho D_i^4 g \bar{r}_{1f} \left\{ \frac{\mathbf{r}_{f,sat}^{sec} \mathbf{b} C_p \Delta T_{2f}}{U_{1f}} + \frac{h_{fg}}{U_{2f} \Delta T_{2f}} \left[x_i \mathbf{r}_{f,sat}^{sec} - \frac{1}{v_{fg}} \log \left(1 + \frac{v_{fg}}{v_f} x_i \right) \right] \right\}}{16 D_o (fL/D_i + K)} \quad (22)$$

When the inlet quality x_i in Eq. (22) is zero, Equation (22) is reduced to Eq. (21).

Comparing Eq. (21) with Eq. (22), it can be seen that the characteristic flow for two-phase case is greater than that for single-phase case. Thus, two-phase case is less stable than single-phase case in terms of flow excursion instability.

3. Flow Behavior in Multiple U-tubes

As mentioned earlier, a UTSG has several hundreds or thousands of vertical, inverted U-tubes, of which the tube lengths are different. The different tube lengths yield different pressure drop characteristic curves. However, since all the U-tubes are connected to the same inlet and exit plenums in common, they experience the same pressure drop. This causes the heterogeneous flow behaviors in the multiple U-tubes.

Consider a quasi steady state in a UTSG with two – short and long - U-tubes, which is shown in Fig. 5(a). Figure 5(b) illustrates the pressure drop-flow rate characteristics of the tubes. It is assumed that, initially, the flows in the two tubes are in positive direction. Then, gradually decreasing the pressure drop ($P_{inlet} - P_{exit}$), the flow behaviors in short and long U-tubes will be:

- (a) $\dot{m}_{short} > \dot{m}_{long} > 0$ when $P > dP_A$,
- (b) $\dot{m}_{short} > 0$ and $\dot{m}_{long} < 0$ when $dP_C \leq P < dP_A$,
- (c) $\dot{m}_{short} < \dot{m}_{long} < 0$ when $P < dP_C$,

where dP_A and dP_C are defined in Fig. 5(b). The case (b) is one of the situations that were observed in the LSTF experiments [2, 3].

In order to verify the flow behaviors explained above, three conceptual transients in a UTSG with two U-tubes are simulated using the best-estimate system code MARS [8]. In the conceptual problem, the lengths of short and long tubes are 18 m and 20 m, respectively. The tubes' inner diameter is 0.01692 m, of which thickness is 0.0011 m. The primary side pressure (at the exit) is 15 MPa. The secondary side is saturated at a pressure of 6.95 MPa (saturated temp. 558.5 K).

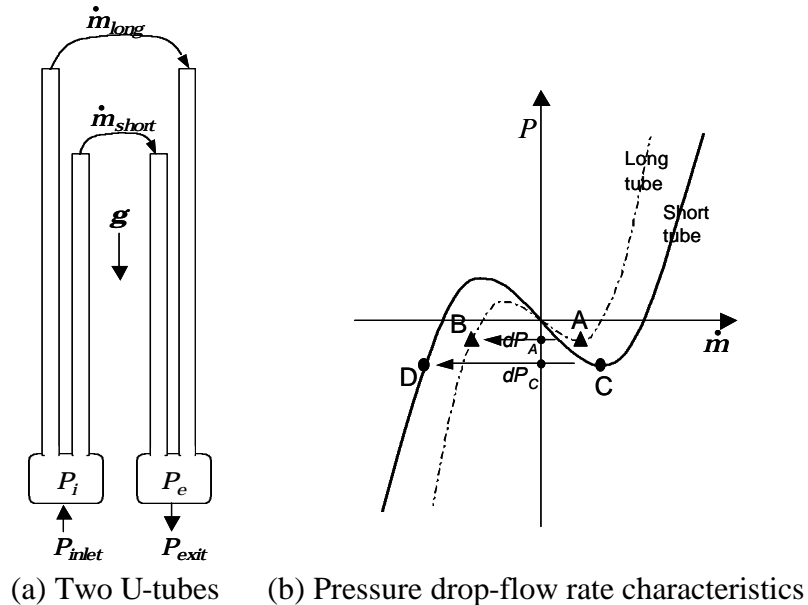


Fig. 5. The primary side of a steam generator with two U-tubes.

For the MARS simulation, two “single volumes” were used to model the inlet and exit plenums. The short and long tubes were modeled with “pipe” components with 18 and 20 “volumes,” respectively. To provide boundary conditions, “time dependent volumes” were attached to the inlet and exit plenums. The secondary side was modeled with a very big “pipe” component. To simulate the primary-to-secondary heat transfer, two “heat structure” models for the short and long tubes were used.

3.1 “Inlet Pressure and Exit Pressure” Boundary Conditions

Two inlet flow conditions are used: (i) subcooled water at a temperature of 598 K, and (ii) two-phase mixture with an equilibrium quality of 0.05. The pressure at the exit plenum is 15 MPa in common.

The transient is initiated by changing the inlet pressure as a function of time; the resulting pressure difference between the inlet and exit boundary volumes ($P_{inlet} - P_{exit}$) is shown in Fig. 6. The calculated mass flow rates for single- and two-phase cases are given in Figs. 7 and 8, respectively. Mark **A** in Figs. 7 and 8 represents the positive-to-negative flow excursions, whereas mark **B** indicates negative-to-positive flow excursions with hysteresis.

Figure 9 shows the phase diagram of pressure difference vs. mass flow rate during the transient. Due to the fluid inertia, the timings of flow reversals and the characteristic flows of the two tubes are not clearly distinguished. However, the existence of flow excursions is clearly shown.

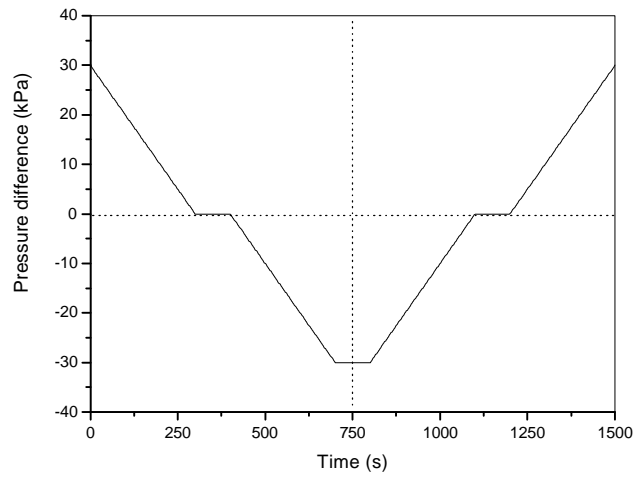


Fig. 6. Pressure difference versus time (Boundary condition).

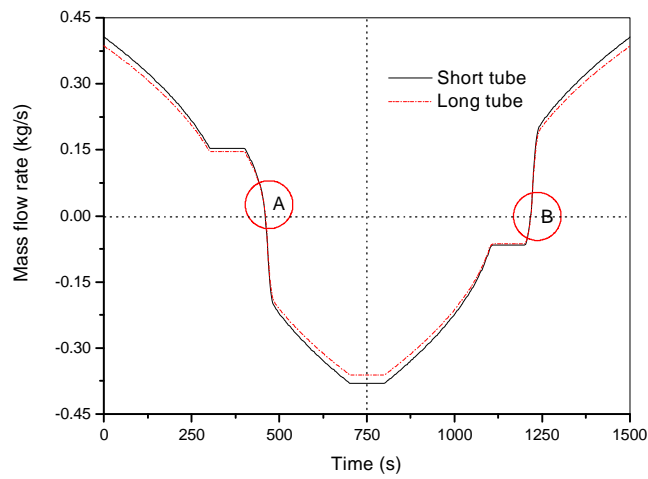


Fig. 7. Transient mass flow rates in short and long tubes: single-phase case.

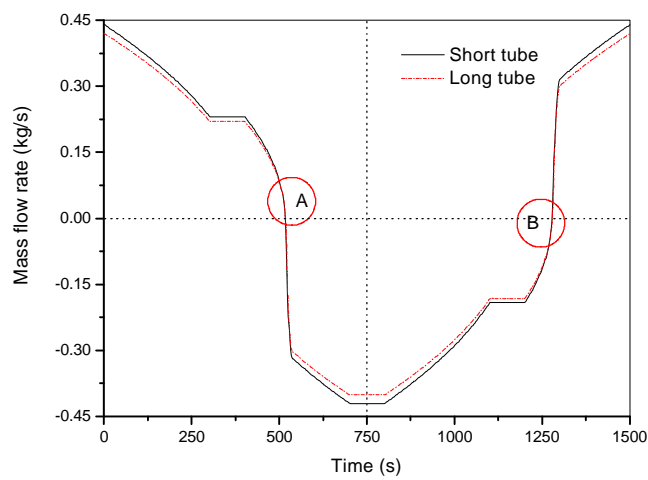


Fig. 8. Transient mass flow rates in short and long tubes: two-phase case.

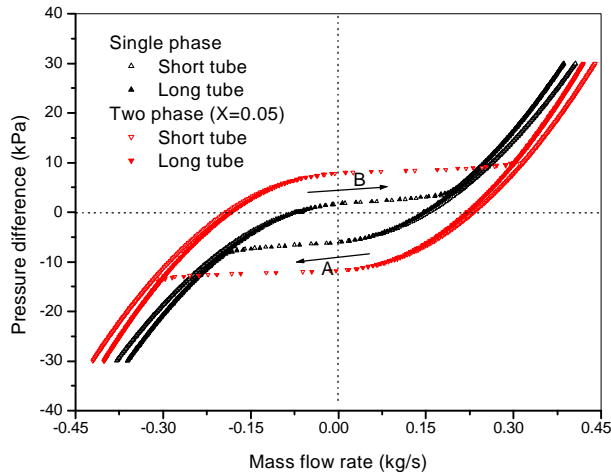


Fig. 9. Pressure difference versus flow rate during the transient (See mark A and B in Figs. 7 and 8).

3.2 “Inlet Flow Rate and Exit Pressure” Boundary Conditions

An additional flow transient is simulated with “inlet flow rate and exit pressure” boundary conditions. The transient is initiated by changing the inlet mass flow rate as a function of time, which is given by blue dashed line in Fig. 10. Inlet temperature is 598 K (subcooled water). The secondary-side conditions are the same with those of the previous problems.

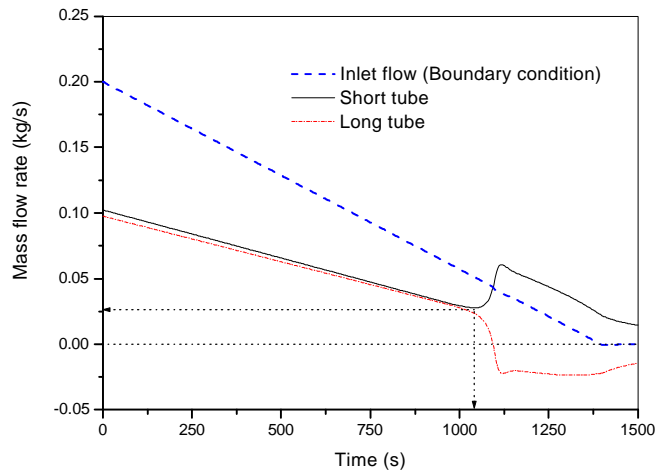


Fig. 10. Mass flow rates versus time (Inlet flow boundary condition).

In Fig. 10, the calculated mass flow rates in the short and long tubes are illustrated. As the inlet flow rate decreases, they also decrease. However, reaching a critical point, flow excursions occur, that is, the flow in the long tube is reversed, whereas the flow in the short tube suddenly increases. The results are similar to the reversed flow in the longer U-tubes of the LSTF experiments.

According to Eq. (21), the characteristic flow rates are approximately 0.023 kg/s and 0.021 kg/s for the short and the long tubes, respectively. It can be seen in Fig. 10 that the sudden

change occurs when the mass flow rates of the two tubes reach around 0.026 kg/s. Therefore, the characteristic flow rate in Eq. (21) is reasonably accurate.

4. Conclusions

The flow in the primary side of a UTSG was analyzed in terms of static instability. Using a one-dimensional, integrated flow model, the characteristic flow of a U-tube was derived for single- and two-phase flow cases. When the U-tube flow decreases below the characteristic flow, a flow excursion will occur, resulting in flow reversal. Generally, the design flow rate of a U-tube is far greater than the characteristic flow and, thus, the flow excursion will not occur during normal operating conditions. However, under natural-circulation conditions, the flow excursion may occur. Especially, two-phase flow is less stable than single-phase flow in terms of flow excursion instability.

Nomenclature

A	Flow area of a U-tube [m^2],
C_p	Specific heat [J/kg K],
D	Inner diameter of the U-tube [m],
f	Friction factor [dimensionless],
g	Gravitational acceleration [m/sec^2],
H	Height [m],
L	Tube length [m],
K	Local form loss factor [dimensionless],
\dot{m}	Mass flow rate in a U-tube [kg/sec],
P	Pressure [Pa],
s	Coordinate along the U-tube [m],
t	Time [sec],
T	Coolant temperature [K],
U	Overall heat transfer coefficient across the tube wall [$\text{W/m}^2 \text{K}$],
V	Velocity [m/sec].

Greek Symbols

β	Thermal expansion coefficient [K^{-1}],
P	Pressure drop [Pa],
ρ	Density [kg/m^3].

Subscripts

$1f$	Single phase,
$2f$	Two phase,
c	Characteristic,
f	Saturated water,
g	Saturated steam,
i	Inlet or inner,
e	Exit,

o Outer,

Superscripts

pri Primary side,

sec Secondary side.

Acknowledgement

This work has been performed as a part of the Nuclear R&D Program supported by Ministry of Science and Technology (MOST) of the Republic of Korea.

References

1. B. E. Boyack, Survey of Natural-circulation Cooling in U. S. Pressurized Water Reactors, *Nucl. Sci. Engrg* **91**, 248-261 (1985).
2. Y. Kukita, H. Nakamura, and K. Tasaka, Nonuniform Steam Generator U-tube Flow Distribution During Natural Circulation Tests in ROSA-IV Large Scale Test Facility, *Nuclear Science and Engineering*, **99**, pp. 289-298 (1988).
3. F. Serre, "CATHARE Calculations of LSTF Experiments in JAERI," Presented at CATHARE Technical Meeting, Commissariat a l'Energie Atomique - Grenoble, December 11, 1990, Grenoble, France.
4. T. Tasaka, Y. Kukita, Y. Koizumi, M. Osajabe, and H. Nakamura, "The results of 5% small-break LOCA tests and natural circulation tests at the ROSA-IV LSTF," *Nuclear Engineering and Design* **180**, 37-44 (1988).
5. B. Noel, and R. Deruaz, "Reflux condensation with nitrogen in steam generator U-tubes analysis of BETHSY test 7.2c using CATHARE code," 3rd Intl. Symposium on Multiphase Flow and Heat Transfer, Xi'an, China, Sep. 19-21, 1994.
6. W. H. Strohmayer, Dynamic Modeling of Vertical U-tube Steam Generators for Operational Safety Systems, PhD Thesis, The Department of Nuclear Engineering, Massachusetts Institute of Technology, 1982, pp. 4-19 ~ 4-25.
7. M. M. Padki, K. Palmer, S. Kakac, and T. N. Veziroglu, "Bifurcation analysis of pressure-drop oscillations and the Ledinegg instability," *International J. Heat and Mass Transfer* **35**(2), 525-532 (1992).
8. J.-J. Jeong, K.S. Ha, B.D. Chung, W.J. Lee, "Development of A Multi-dimensional Thermal-Hydraulic System Code, MARS 1.3.1," *Annals of Nuclear Energy* **26**(18), 1161-1642 (1999).